Int. J. Electrochem. Sci., 13 **(2018)** 12085 – 12098, doi: 10.20964/2018.12.60

International Journal of
ELECTROCHEMICAL
SCIENCE
www.electrochemsci.org

Effect of the Competitive Adsorption of Borate and Chloride Ions on the Breakdown Potential of Iron

Yuting Zhou, Tianpeng Wen, Endong Jin, Danbin Jia, Feixiong Mao[*], *Jingkun Yu*[*]

School of Metallurgy, Northeastern University, Shenyang 110819, China
[*]E-mail: maofx@mail.neu.edu.cn, yujk@mail.neu.edu.cn

Received: 25 August 2018 / *Accepted:* 4 October 2018 / *Published:* 5 November 2018

The effect of $\frac{a_{Cl^-}}{a_{B(OH)_4^-}}$ on the passivity breakdown for pure iron in borate buffer solution containing chloride ions has been studied and the results also have been analyzed using the Point Defect Model (PDM). The results showed that boric acid acts as an inhibitor for passivity breakdown of iron in chloride-containing solution. The critical areal vacancy concentration that leads to the breakdown of the passive film is estimated to be $\leq 2.17\times10^{15}$ cm^{-2} experimentally, which is consistent with the value （$10^{14}-10^{15}$ cm^{-2}）calculated from the structural information of substrate Fe and Fe_2O_3 barrier layer. The distributions of the critical breakdown potential, as determined experimentally in the chloride-containing solutions having different concentrations of borate, are near normal, while the cumulative probability distributions are consistent with those calculated from the PDM.

Keywords: Iron; Passivity breakdown; Point Defect Model; Borate inhibition.

1. INTRODUCTION

When chemically active metals (except for those, such as gold, and silver) are used in certain environments (non-aggressive), a stable passive film may can form on their surfaces, which can reduce the corrosion rate and prolong the service life of metals to a certain degree. The passive film on the metal has a thickness of not more than tens of atomic diameters. When the passive film is being destroyed, the metal beneath the passive film reacts with the environment faster than usual and has a negative effect on the service time of the metal. When the electrolyte in contact with the metal contains aggressive ions, (such as, Cl^-) passive film on the metal easily suffers with localized attack, for example, pitting corrosion [1]. Passivity breakdown occurs in several steps, including the pit nucleation, growth, and the repassivation [2]. Therefore, understanding the mechanism of passivity breakdown, especially when the metal is simultaneously exposed to both corrosive and inhibitive environments is very important.

Iron based alloys are one of the most widely used alloy materials and the compositions and electronic characteristics of the passive film on iron have extensively been studied [3-6]. Researchers have also studied adding various inhibitors to improve the breakdown potential for iron in borate buffer solutions, and the competitive adsorption of inhibitive ions and aggressive ions [7-12]. Boric acid was used to prepare the borate buffer solution to maintain a stable pH value within the buffer range. However, few studies have been conducted to study the effect of borate on the passivity breakdown of iron in chloride-containing borate buffer solution. The boron species existed in the borate buffer solution also seems complicated. Yang [7] found that the concentration of boric acid may affect the breakdown potential of 316SS which means that borate may not be an inert electrolyte in passivity study. Therefore, in this paper, the potential of borate to act as an inhibitor for iron in borate buffer solution containing chloride was studied, and the influence of $[Cl^-]/[H_3BO_3]$ on the passivity breakdown of pure iron was analyzed. In addition, the mechanism of passivity breakdown for iron in chloride-containing borate buffer solutions according to the Point Defect Model (PDM) was also explored briefly.

2. EXPERIMENTAL

A typical three electrode cell used for the electrochemical measurement is shown in Fig.1. The tightness of the flask was assured by the rubber stoppers. The working electrode (WE) was an iron (99.5%) rod embedded with the epoxy resin with a 0.0314cm^2 working area. Then the working surface of WE was abraded with SiC papers and given a mirror polish using diamond suspension. In this study, a platinum gauze and a saturated camel electrode connected to a Luggin capillary probe were served as the counter electrode (CE) and the reference electrode (RE), respectively.

All the chemicals used were analytical reagent grade (AR) and the solutions used in this study were prepared by dissolving the AR chemicals in deionized water. Different electrolytes were obtained by changing the concentrations of boric acid and chloride. The pH of the buffer solutions was adjusted by adding NaOH in different concentrations. Before each experiment, the electrolytes were exhausted with high purity nitrogen (99.99%) for 2 hours, and during the experiment, a small flux of N_2 was maintained to keep the electrolytes being saturated with N_2.

The electrochemical measurements were performed using a Gamry electrochemical system at ambient temperature (22 ± 2 $^\circ$C). Cyclic potentiodynamic polarization experiments were carried out at a positive going voltage scan rate of 0.1667mV/s and at a negative going scan rate of 1 mV/s. Each experiment was repeated for 3 times. After the potentiodynamic polarization experiments, the surface of iron was cleaned with deionized water and then was been dried. After being polarized, the surface of iron was observed using an optical microscope (OM, Olympus DSX500).

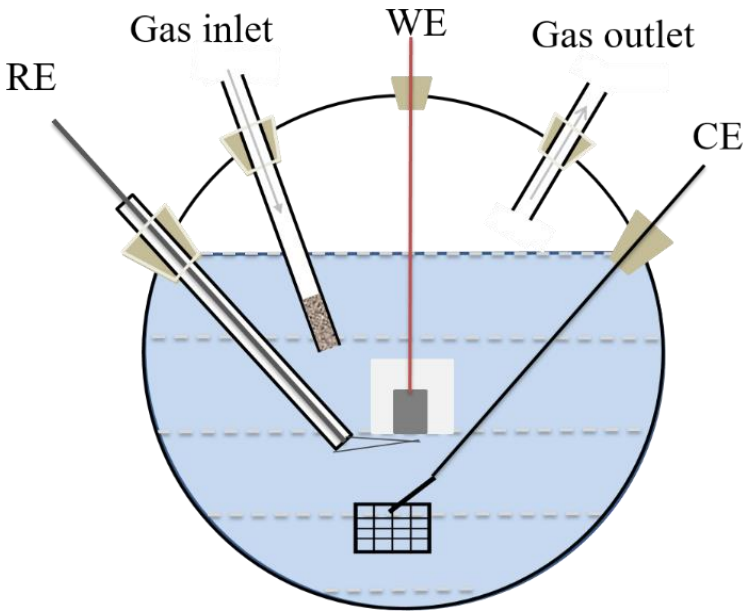

Figure 1. Schematic diagram of a three electrode cell

3. RESULTS AND DISCUSSION

Fig. 2 - Fig. 4 show the potentiodynamic polarization curves for pure iron in different concentrations of boric acid (BA) in buffer solutions containing chloride ions with NaOH added to maintain the pH at 8.4 ± 0.2. The arrows in Fig. 2 represent the scanning directions. The polarization curves show relatively flat passive regions followed by a dramatic increase in the current density corresponding to passivity breakdown. Therefore, the potential at which the current density suddenly increases was defined as the breakdown potential (V_c). The occurrence of passivity breakdown was confirmed by reversing the potential sweep and observing the typical hysteresis that is diagnostic of breakdown. Noted that when the solution contained a higher chloride concentration (such as, 0.5 M in this study), the passive region was not obvious, but there still existed a point representing the breakdown potential where the current density increased suddenly (see Fig. 3). If the [Cl^-] in solution continuously increased (such as, to a value of 1 M), no passive region was observed for the poor corrosion resistance of pure iron in this solution (see Fig. 4). The breakdown potential increased significantly with the increase of boric acid concentration under constant [Cl^-] and pH. The results demonstrate that boric acid can act as an inhibitor of the breakdown of passive film on copper in chloride-containing solutions, indicating that borate ions are the inhibiting species. This can also be demonstrated using the results presented in Fig. 5 which displays the images of the surface of iron after cyclic polarization. With more boric acid added into chloride-containing solutions, the corrosion of the iron surface obviously decreased. Table 1 presents the breakdown potential for iron in chloride-containing borate buffer solutions (pH=8.4±0.2).

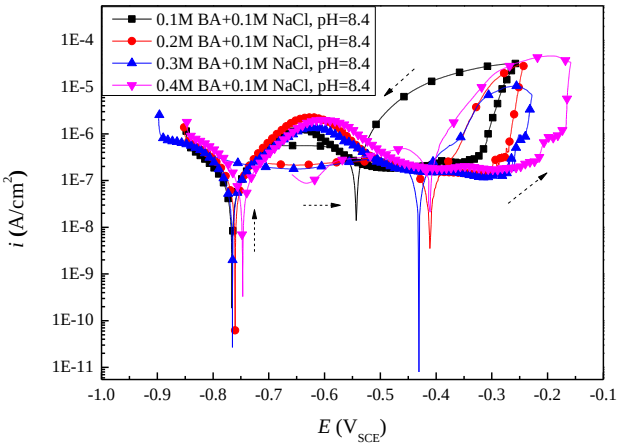

Figure 2. Cyclic potentiodynamic polarization curves for iron in 0.1 M chloride-containing borate buffer solutions with different boric acid concentrations (pH=8.4±0.2).

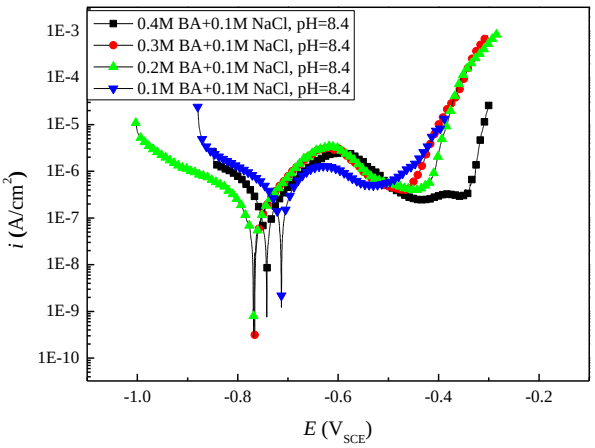

Figure 3. Potentiodynamic polarization curves for iron in 0.5 M chloride-containing borate buffer solutions with different boric acid concentrations (pH=8.4±0.2).

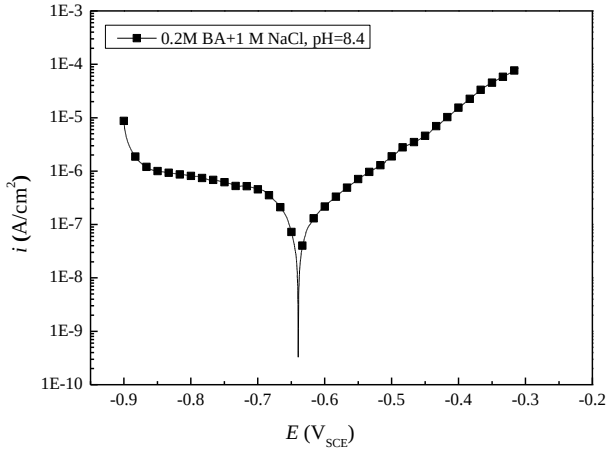

Figure 4. Potentiodynamic polarization curves for iron in 0.2 M borate buffer solution containing 1 M chloride (pH=8.4±0.2).

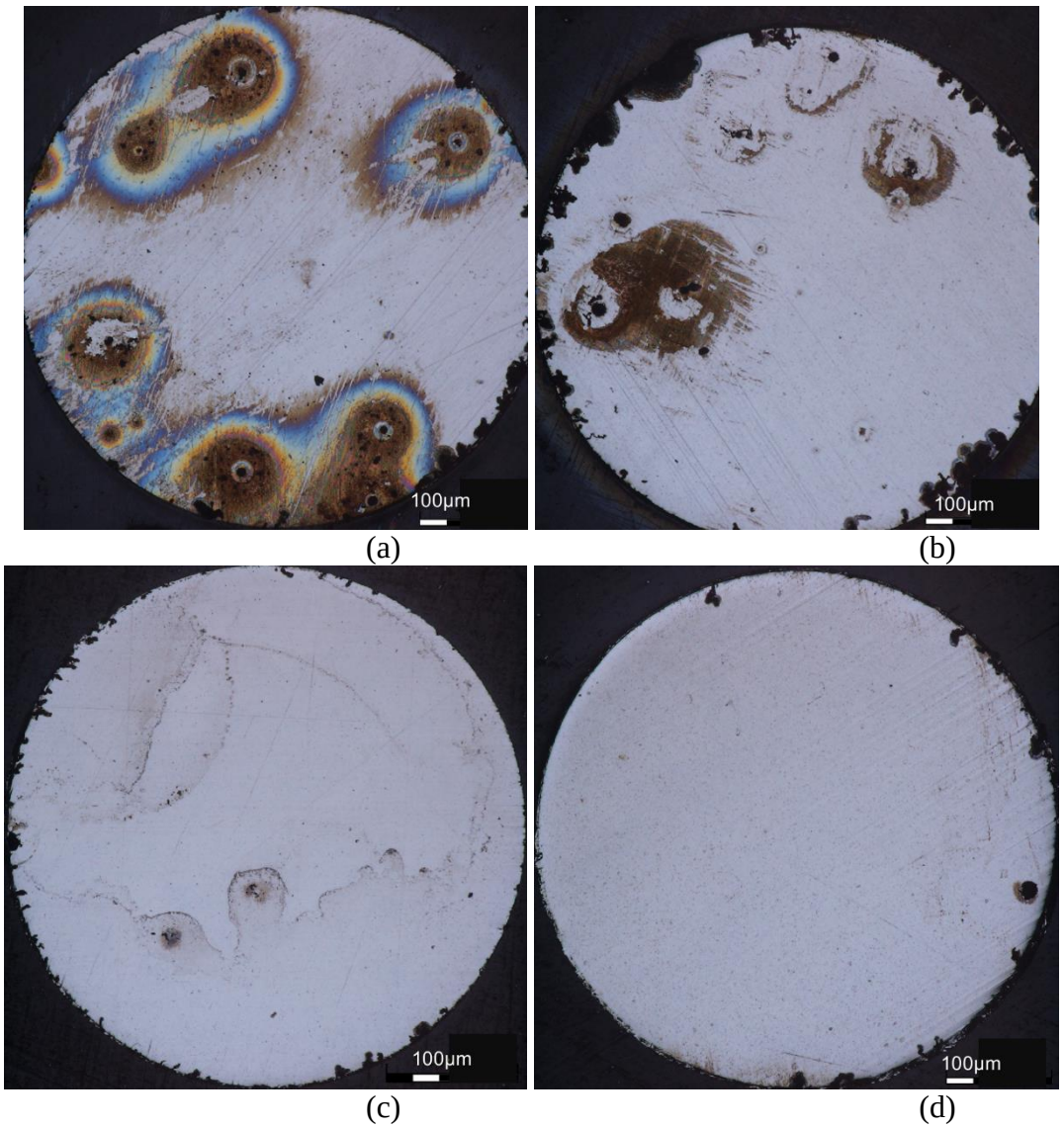

Figure 5. Photographs for the surface of iron after cyclic potentiodynamic polarization, pH = 8.4 ± 0.2. (a) 0.1M NaCl +0.1M BA, (b) 0.1M NaCl +0.2M BA, (c) 0.1M NaCl +0.3M BA, (d) 0.1M NaCl +0.4M BA

Table 1. Breakdown potential for iron in borate buffer solutions containing chloride (pH=8.4±0.2)

	0.018M Cl^-	0.05 M Cl^-	0.1 M Cl^-	0.5 M Cl^-
0.1M BA	-0.221V_{SCE}	-0.288V_{SCE}	-0.333 V_{SCE}	-0.533V_{SCE}
0.2M BA	-0.139 V_{SCE}	-0.199 V_{SCE}	-0.262 V_{SCE}	-0.471 V_{SCE}
0.3M BA	-0.100 V_{SCE}	-0.165 V_{SCE}	-0.211 V_{SCE}	-0.415 V_{SCE}
0.4M BA	0.030 V_{SCE}	-0.145 V_{SCE}	-0.194 V_{SCE}	-0.360 V_{SCE}

Significant research [11, 12] has been reported on the relationship between passivity breakdown on metals and alloys and the identities of the aggressive (X^-) and inhibitive anions (A^{n-}). A logarithmic relationship between V_c and activities of the X^- and A^{n-} based upon the concept of competitive absorption into surface oxygen vacancies is given as Eq. (1) [7].

$$V_c = V_0 - b \times \log(\frac{a_{X^-}}{a_{A^{n-}}}) \quad (1)$$

where b is a constant having a value that depends upon the type of the inhibiting and aggressive anions. In the present work, chloride ion and borate anion are the aggressive anion (X^-) and the inhibitive anion (A^{n-}), respectively. In the chloride-containing borate buffer solutions (pH = 8.4), the boron species may exist in the forms of $B(OH)_4^-$, $B_2(OH)_7^-$, $B_3(OH)_{10}^-$, $B_4(OH)_{14}^{2-}$, and among these borate anions, $B(OH)_4^-$ accounts for the majority of the boron species [7]. In order to estimate the value of b, the breakdown potential must be plotted as a function of $a_{X^-}/a_{A^{n-}}$, as obtained. $B(OH)_4^-$ (or BO_2^-) is an oxyanion capable of being absorbed in an oxygen vacancy and competes with the chloride ions. Considering the ionic strength/activity coefficient effects, the activity of $B(OH)_4^-$ can be calculated using the Debye–Hückel equation. In addition, considering the effect of chloride on the boron species, the relationship between breakdown potential and $a_{B(OH)_4^-}$ under different values of fixed [Cl^-] was analyzed, and the results are shown in Fig. 6. The four values of the slope demonstrate that the concentration chloride ions affected the forms of boron species or the concentration of $B(OH)_4^-$. The slope of the linear fit of 0.018 M chloride-containing borate buffer solution was higher than the other three slope values, which indicates that when the electrolyte contained a low chloride concentration, adding more borate acid can improve the iron breakdown potential effectively. When the chloride concentration was further increased (0.05 M, 0.1 M, 0.5 M), similar trend in slope values was observed, suggesting that under these chloride concentrations, the effect of chloride on the boron species was generally similar. Therefore, the borate can no longer be seen as the inert electrolyte in this study, but can act as an inhibitor competing with the chloride for iron, which can be demonstrated by the improved breakdown potential with respect to the increased boric acid concentration, especially in low concentration of chloride. The breakdown potential as a function of $\frac{a_{Cl^-}}{a_{B(OH)_4^-}}$ is depicted in Fig. 7. The chloride concentration lies within the range from 0.05 M to 0.5 M and the relationship is determined as Eq.(2).

$$V_c = -0.361 - 0.259 \times \log(\frac{a_{Cl^-}}{a_{B(OH)_4^-}}) \quad (2)$$

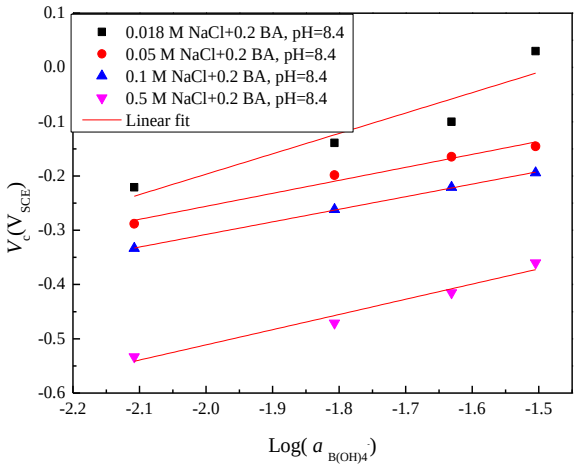

Figure 6. The breakdown potential as a function of the activity of borate ion

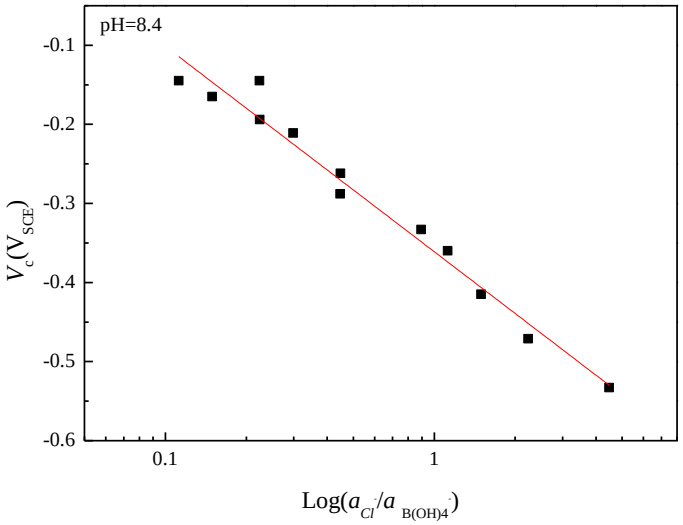

Figure 7. The breakdown potential as a function of $\frac{a_{Cl^-}}{a_{B(OH)_4^-}}$

The PDM [13] gives a quantitative relationship between V_c and pH and chloride activity of electrolyte, as given by Eq. (3). Noted that the concentration of inhibition is a constant and the pH is adjusted by adding NaOH.

$$V_c = V_0 - \frac{\beta}{\alpha} pH - \frac{2.303RT}{\alpha F} \times \log(a_{Cl^-}) \quad (3)$$

where α and β denote the dependence of potential drop across the barrier layer/ solution (bl/s) interface on applied potential and pH of electrolyte, respectively. The borate has no effect on the forms of chloride in electrolyte. In this study, it was assumed that the value of $\frac{2.303\mathrm{RT}}{\alpha F} \times \log a_{B(OH)_4^-}$ related to the chloride has an influence on V_0 in Eq. (3) rather than on the slope.

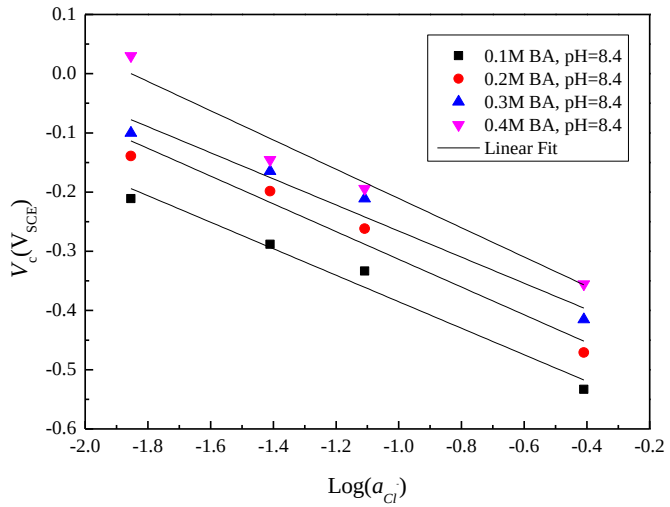

Figure 8. Breakdown potential for iron as a function of chloride activity in fixed boric acid (pH=8.4±0.2).

This can also be estimated from the similar slope values obtained from the fitting lines shown in Fig. 8. Fig. 8 shows the breakdown potential as a function of activity of chloride at a constant pH of electrolyte with different fixed boric acid concentrations. Fig. 9 gives the relationship between breakdown potential and the pH of electrolyte obtained in 0.1 M chloride concentration and in 0.5 M chloride concentration, respectively. The values of parameters, α and β were determined to be 0.25 and -0.039V, respectively. The V_0 Eq. (3) values were calculated to be -1.819V and -1.783V from Fig.8 and Fig.9 (0.2M BA+0.1M NaCl, pH=8.4±0.2), respectively. The two similar values of V_0 suggest that the PDM gives a reasonable description for passivity breakdown on iron with regard to the dependencies of breakdown potential on the chloride activity and pH of electrolyte [Eq. (3)].

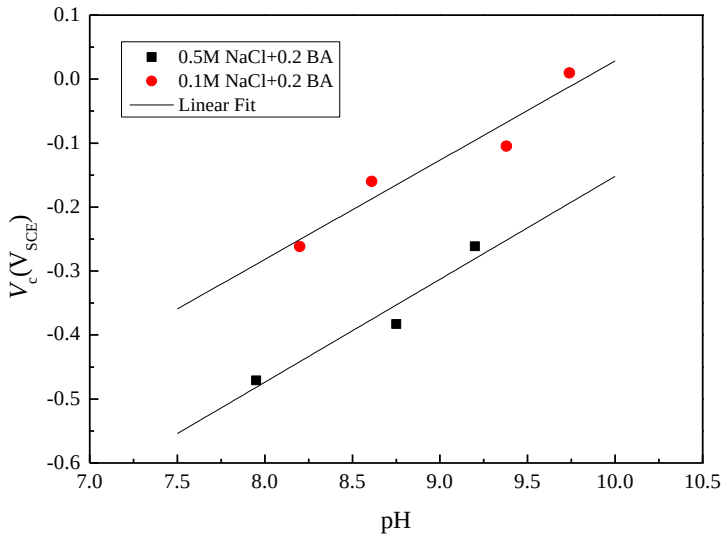

Figure 9. Breakdown potential for iron as a function of pH of electrolyte.

Researchers [14, 15] have found that under potentiodynamic polarization conditions, the measured breakdown potential was related to the voltage scan rate. The measured breakdown potential usually increased with the increasing voltage scan rate. Haruna and Macdonald [15] raised an analytical relationship between the critical breakdown potential and the square root of the voltage scan rate, as given in Eq. (4). This quantitative relationship was confirmed by many experiments [15-20].

$$V_c(v) = (\frac{2\xi RT}{\chi\alpha F J_m})^{1/2} v^{1/2} + V_c(v=0) \quad (4)$$

where V_c (v = 0) is the standard breakdown potential V_c^0, which can be obtained under potentiostatic polarization condition at a potential scan rate of 0 mV/s. F is Faraday's constant, χ is the oxide state of cation in barrier layer (χ =3, the barrier layer is assumed to be Fe_2O_3 [19]). J_m is the annihilation rate of cation vacancies at metal/barrier layer (m/bl) interface. ξ, which is the critical vacancy areal concentration (#.cm^{-2}) can be obtained from the slope of the plot in Fig. 9.

Fig. 10 depicts the dependence of critical breakdown potential on the voltage scan rate for iron in 0.2M borate buffer solution and 0.3M borate buffer solutions containing 0.1 M NaCl with a pH of 8.4±0.2. Noted that, in this study, considering that when the voltage scan rate was sufficiently high, the passive film on the substrate iron may be thin and weak and can't be formed very well in a short

time, under the increased high applied voltage, the iron easily underwent passivity breakdown. Due to this reason, the maximum voltage scan rate was only up to 5 mV/s.

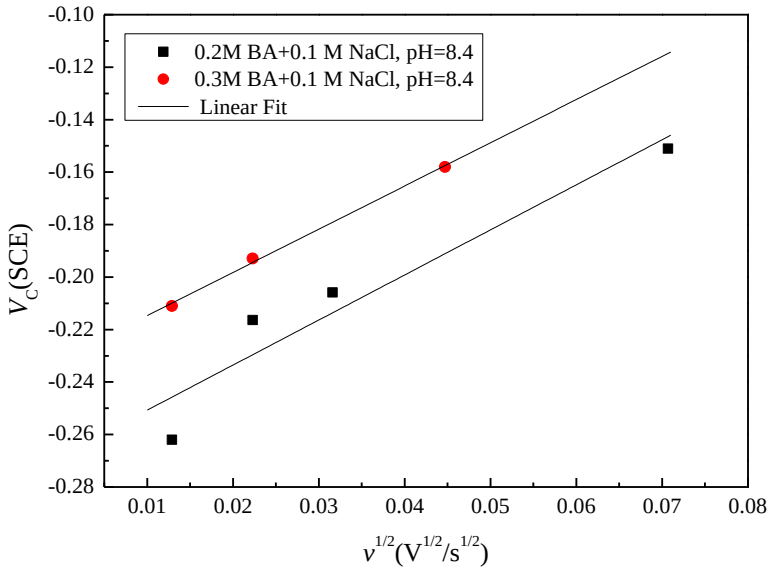

Figure 10. The relationship between the critical breakdown potential and the square root of voltage scan rate.

The PDM [13, 21, 22] considers that the barrier layer formed on the metal or alloy is a pointed defected layer with cation interstitial, oxygen and cation vacancy. The cation vacancies generated at barrier layer/solution (bl/s) interface, migrate to the metal/barrier layer (m/bl) interface under the effect of the electric filed within the barrier layer, and are annihilated by cation ejection into the barrier layer from substrate metal. If the flux of cation vacancies towards to m/bl interface (J_{ca}) exceeds J_m, cation vacancies cannot be annihilated promptly, and hence, condensate at m/bl interface. When the condensed areal vacancy concentration exceeds a critical value (ξ, cm^{-2}), the barrier layer separates from the substrate locally and a blister is formed. The existence of blister prevents the growth of barrier layer into the substrate. Continued dissolution of the bl at the bl/s interface and expansion of the blister due to continued condensation of cation vacancy at the outer edge of the blister causes the thinning and expansion of the barrier layer "cap" over the vacancy condensation point eventually resulting in the rupture of the cap over the condensate, marking a meta-stable passivity breakdown event [16, 17]. The quantity, ξ, which denotes the critical areal concentration of vacancy condensation (#. cm^{-2}) at the m/bl interface, is related to the structures of the barrier layer and substrate metal, depending on whether the vacancies condense on the barrier layer cation sublattice or on the metal lattice [16,17]. Thus, assuming that detachment of the barrier layer from the substrate metal demands vacancy condensation on all interfacial sites on the cation sublattice of the barrier layer or upon all interfacial sites of the metal lattice, the ξ value is conveniently calculated from the respective crystal structures. When passivity breakdown occurs, the current density resulting from the migration of cation vacancies should be less than the measured current density (I_{ss}) [16].

$$J_m < \frac{I_{ss} N_A}{\chi F} \quad (5)$$

The maximum value of I_{ss} was estimated to be 6 μA·cm^{-2} experimentally when the iron was in electrolytes which have different concentrations of chloride and different values of pH. The value of ξ was calculated to be ξ <2.17×10^{15} cm^{-2} from the slope of fitting line in Fig. 10. The value of ξ can also be obtained from the structures of the substrate iron and barrier layer Fe_2O_3 depending on whether the vacancies condense on metal lattice or on cation sublattice of the barrier layer. The areal atomic densities of Fe atoms are about 10^{14} cm^{-2} for the barrier layer Fe_2O_3 and 10^{15} cm^{-2} for the substrate metal iron, which are in consistent with the value obtained from the relationship between the breakdown potential and the voltage scan rate.

The experiments in Fig. 2 were repeated 20 times to obtain the experimental cumulative probability [$P(V_c)$] for iron in chloride-containing buffer solutions with different concentrations of boric acid, and the results are shown in Fig. 11. The PDM postulates that the breakdown potential sites follow a near normal relationship with regard to the cation vacancy diffusivity (D). The cumulatively probability in critical breakdown potential is given as Eq. (6), where $P(V_c)$ denotes the percentage of potential breakdown sites that have activated at V_c. A more detailed introduction of $P(V_c)$ according to the PDM can be found in the works of Macdonald and his co-workers [23-25].

$$P(V_c) = 100 \times \frac{\int_{-\infty}^{V_C} (\frac{dN}{dV_c}) dV_c}{\int_{-\infty}^{+\infty} (\frac{dN}{dV_c}) dV_c} \quad (6)$$

$$\frac{dN}{dV_c} = \frac{-\gamma' D}{\sqrt{2\pi} \cdot \sigma_D} \times \exp[-(\frac{D - \overline{D}}{\sqrt{2} \cdot \sigma_D})^2]$$

$$= \frac{-b\gamma'}{\sqrt{2\pi} \cdot \sigma_D \cdot a_{Cl^-}^{\chi}} \times \exp[\frac{-(e^{-\gamma' V_c} - e^{-\gamma' \overline{V_c}})^2 b^2}{2\sigma_D^2 a_{Cl^-}^{\chi}}] \times \exp(-\gamma' V_c) \quad (7)$$

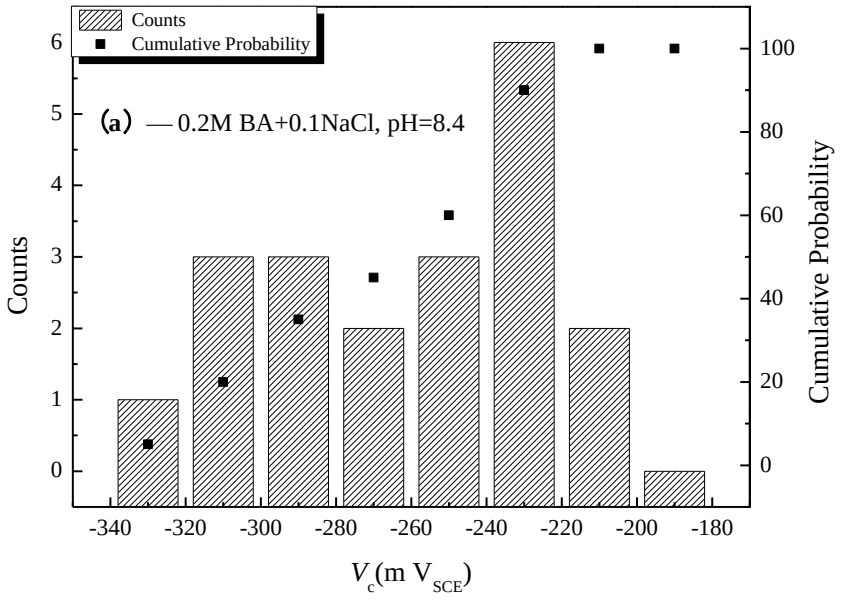

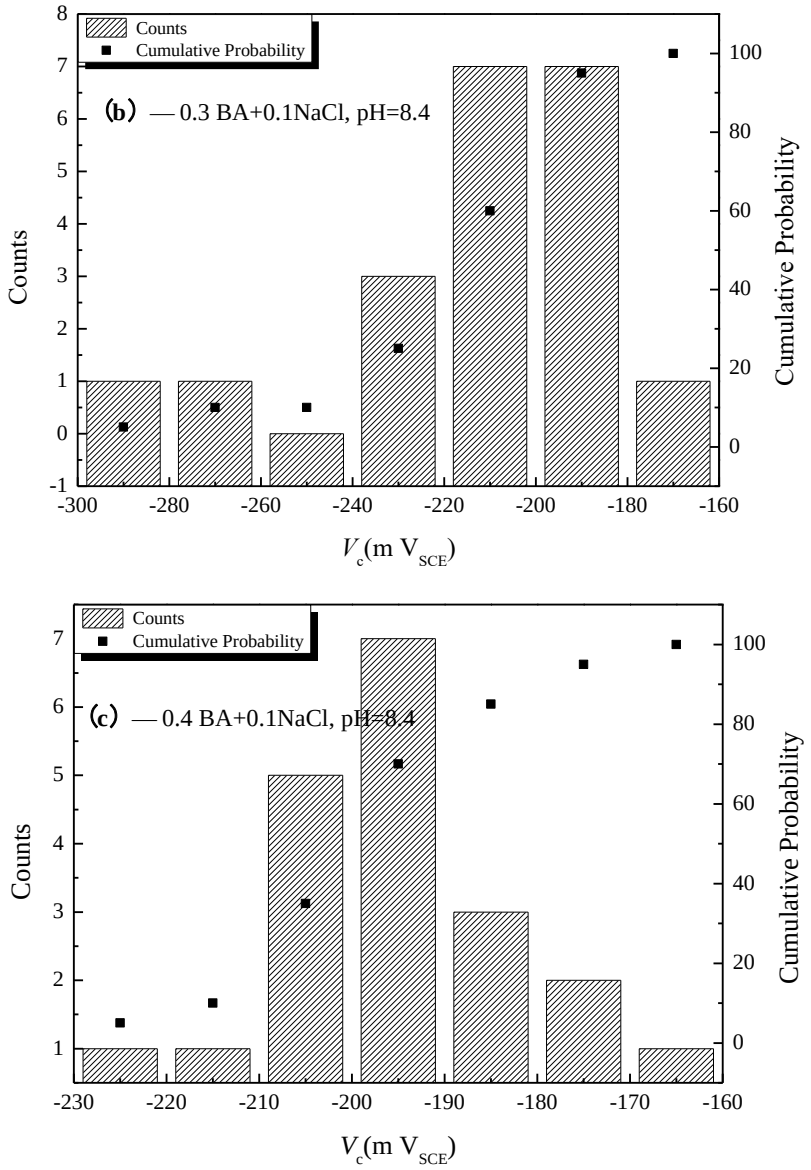

Figure 11. Statistical and cumulative plots of critical breakdown potential for iron, where (a) was in 0.1M NaCl +0.2M BA, (b) was in 0.1M NaCl +0.3M BA, and (c) was in 0.1M NaCl +0.2M BA, respectively (pH=8.4).

Table 2. Parameter values used in calculating $P(V_c)$ in the breakdown potential for iron in deaerated chloride-containing borate buffer solutions (pH=8.4±0.2)

Parameter	Value	Units	Source
T, the absolute temperature	295.15	K	Defined
χ, the barrier layer stoichiometry(Fe_2O_3)	3	Elementary charge	Defined
Ω, the molar volume of Fe_2O_3 per cation	15.23	cm^3/mol	From density
ε, the electric field strength	3×10^6	V/cm	Ref.19

J_m, the annihilation rate of cation vacancies at the m/bl interface	1.24×10^{13}	No./(cm^2·s^1)	Calculated
ξ, the critical areal cation vacancy concentration	2.17×10^{15}	No./(cm^2)	From Figure10
$\overline{D}$, the mean cation vacancy diffusion coefficient	5×10^{-19}	cm^2/s	Ref.19
σ_D, the standard deviation for $\overline{D}$	0.2 $\overline{D}$	cm^2/s	Fitted
α, the dependence of $\phi_{f/s}$ on the applied voltage	0.25	-	From Figure8
β, the dependence of $\phi_{f/s}$ on pH	-0.039	V	From Figure9
$\omega = \Delta G_S^0 + \frac{\chi}{2}\Delta G_A^0 - \frac{\chi}{2}F\phi_{f/s}^0$	-44083.3	J/mol	From Figure8

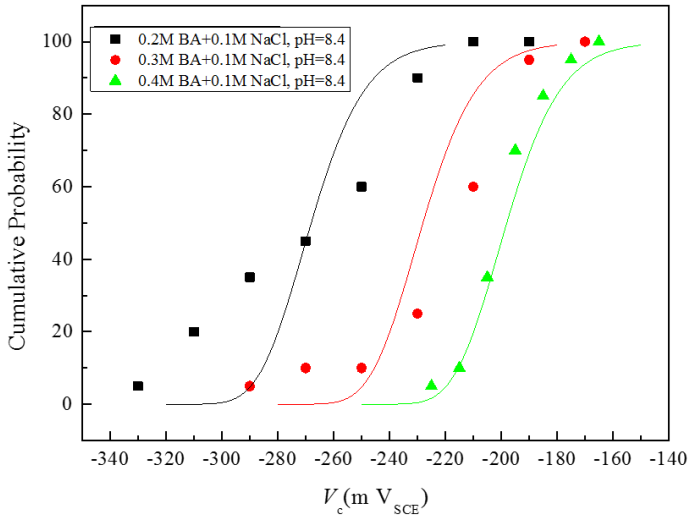

Figure 12. Calculated cumulative probability (solid line) for iron in deaerated 0.1M chloride-containing buffer solutions with different concentration of boric acid.

Table 2 gives the parameter values used in calculating cumulative probabilities in the V_c for iron in deaerated chloride-containing borate buffer solutions obtained from the PDM equations [23-25] and the above experimental data. Thus, cumulative probability of breakdown potential for iron in borate buffer solutions can be calculated by the PDM. Fig. 12 displays the experimental and calculated results for the cumulative probability for iron in buffer solutions with different boric acid concentrations (pH = 8.4, [Cl^-] = 0.1 M). The solid lines were the calculated cumulative probability corresponding to the experimental data plots in Fig.12. Noted that the statistical sample of the experimental data were obtained from the potentiodynamic measurements, which were repeating 20 times. This was done to ensure that the calculated results were satisfied perfectly with the experimental

data. Furthermore, $\sigma_D = 0.2\,\overline{D}$ optimized was used. These parameters values can be used to predict P(V_c) for other boric acid/chloride concentrations and pH. It should be noted that $P(V_c)$ will never be zero even if the potential of electrode becomes infinitely negative as the distribution approaches the co-ordinate axis asymptotically. However, the probability of passivity breakdown becomes vanishingly small.

4. CONCLUSIONS

This work studies the dependence of breakdown potential on the anions in electrolytes, the pH values of electrolytes and the voltage scan rate. Experimental results indicate the validity of the PDM in describing the passivity breakdown of iron in chloride containing borate buffer solutions.

(1) Borate ion acts as an inhibitive ion for iron in passivity breakdown competing with the chloride ion. The breakdown potential decreases linearly with the increasing logarithm of $a_{Cl^-}/a_{B(OH)_4^-}$ at constant pH values.

(2) The values of parameters, which represent the dependence of the potential drop across the barrier layer/ solution interface on the applied voltage and pH of electrolyte, respectively, are determined to be 0.25 and -0.039V by analyzing the relationship between the critical breakdown potential and the chloride activity and pH.

(3) According to the PDM predicting the relationship between critical breakdown potential and voltage scan rate, the critical areal concentration ξ which leads to the passivity breakdown is obtained to be < 2.17×10^{15} cm^{-2} experimentally, which is consistent with the values calculated from geometric structural arguments for Fe and Fe_2O_3 (10^{14} - 10^{15} cm^{-2}).

(4) The experimental cumulative distributions in the breakdown potential for iron in different boric acid solutions are near normal, which is consistent with the quantitative prediction by the PDM.

ACKNOWLEDGEMENTS
The authors acknowledge support of this work by the National Natural Science Foundation of China (51601035), the Fundamental Research Funds for the Central Universities (N162504010)，the China Postdoctoral Science Foundation (No. 2015M581349)， the Ministry of Science and Technology of China (No. 2005DKA10400).

References

1. J. Gulikers, *Mater. Corros.*, 56 (2015) 393-403.
2. D. Sazou, M. Pagitsa, *Chaos Soliton. Frac.*, 17 (2003) 505-522.
3. M. Seo, M. Sato, J. B. Lumsden, *Corros. Sci.*, 17 (1977) 209-217.
4. N. Sato, K. Kudo, *Electrochim. Acta*, 16 (1973) 1909-1921.
5. A. J. Davenport, L. J. Oblonsky, M. P. Ryan, *J. Oral Rehabil.*, 147 (2000) 2162-2173.
6. L. Hamadou, A. Kadri, N. Benbrahim, *Appl. Surf. Sci*., 252 (2005) 1510-1519.
7. S. F. Yang, D. D. Macdonald, *Electrochim. Acta*, 52 (2007) 1871-1879.
8. K. Aramaki, T. Shimura, *Corros. Sci.*, 45 (2003) 2639-2655.
9. E. Fujioka, H. Nishihara, K. Aramaki, *Corros. Sci.*, 38 (1996) 1915-1933.

10. M. Yamaguchi, H. Nishihara, K. Aramaki, *Corros. Sci.*, 36(1994) 241-258.
11. H. H. Strehblow, B. Titze, *Corros. Sci.*, 17 (1977) 461-472.
12. E. McCafferty, *J. Electrochem. Soc.*, 137 (1990) 3731-3737.
13. D. D. Macdonald, *Pure Appl. Chem.*, 71 (1999) 951-978.
14. V. Otieno-Alego, G. A. Hope, H. J. Flitt, *Corros. Sci.*, 33 (1992) 1719-1734.
15. T. Haruna, D. D. Macdonald, *J. Electrochem. Soc.*, 144 (1997) 1574-1581.
16. Y. C. Zhang, D. D. Macdonald, M.Urquidi-Macdonald, *Corros. Sci.*, 48 (2006) 3812-3823.
17. F. X. Mao, C.F. Dong, S. Sharifi-Asl, *Electrochim. Acta*, 144 (2014) 391-399.
18. C. F. Dong, F. X. Mao, S. J. Gao, *J. Electrochem. Soc.*, 163 (2016) C707-C717.
19. S. Sharifi-Asl, F. X. Mao, P. Lu, *Corros. Sci.*, 98 (2015) 708-715.
20. J. Y. Zhong, F. X. Mao, E. Ghanbari, *Electrochim. Acta*, 251 (2017) 324-335.
21. D. D. Macdonald, *Electrochim. Acta*, 71 (1999) 951-978.
22. D. D. Macdonald, *Arab. J. Sci. Eng.*, 56 (2011) 1761-1772.
23. M. Urquidi-Macdonald, D. D. Macdonald, *J. Electrochem. Soc.*, 37 (2012) 1143-1185.
24. M. Urquidi-Macdonald, D. D. Macdonald, *J. Electrochem. Soc.*, 136 (1989) 961-967.
25. D. D. Macdonald, M. Urquidi-Macdonald, *Electrochim. Acta*, 31 (1986) 1079-1086.